Structural Relaxation in PLLA: contribution of different scale motions

Maria Cristina Righetti *[a] and Elisa Mele [b]

[a] National Research Council – Institute for Chemical and Physical Processes (CNR-IPCF), Via Moruzzi 1, 56124 Pisa, Italy. E-mail: cristina.righetti@pi.ipcf.cnr.it

[b] Materials Department, Loughborough University, LE11 3TU, Loughborough, UK

Abstract: The enthalpy relaxation in amorphous and semi-crystalline poly(L-lactic acid) (PLLA) has been investigated at low and high undercooling to identify the different scale motions that contribute to physical ageing, and the temperature ranges in which they are active. The temperature limit below which exclusively small-scale localized motions produce structural relaxation in PLLA has been identified. In addition, motions different from pure cooperative large-scale motions and pure small-scale local rearrangements, localized in the MAF, are found to mainly contribute to structural relaxation at intermediate undercooling. These motions are suggested to be related with the Johari-Goldstein process.

Keywords: Mobile amorphous fraction, Rigid amorphous fraction, Structural relaxation, Cooperative motions, Local motions

1. Introduction

The amorphous phase of semi-crystalline polymers, as poly(L-lactic acid) (PLLA) is constituted by a mobile fraction (MAF), which vitrifies and devitrifies at the bulk T_g, and a rigid fraction (RAF), located at the amorphous/crystal interface, which vitrifies and devitrifies at temperatures higher than the bulk T_g [1]. Both MAF and RAF contribute to structural relaxation upon annealing at temperatures below T_g [2]. It was recently demonstrated that for amorphous and semi-crystalline PLLA, the enthalpy recovered after isochronal annealing ($\Delta h_{a,}$) at different annealing temperatures (T_a) exhibits a markedly asymmetric bell-shape when plotted as a function of the undercooling ($T_g - T_a$), with a pronounced tail on the high ($T_g - T_a$) side [2]. For the semi-crystalline samples, the Δh_a values normalized to the respective mobile amorphous weight fraction, were found to diverge progressively from the amorphous curve by increasing the undercooling [2]. This behaviour was rationalized by

1

assuming that also RAF takes part in the enthalpy relaxation, with a contribution that becomes recognizable at high undercooling. RAF does not take part into the cooperative segmental motions around T_g, and can participate in the structural relaxation only through small-scale conformational rearrangements, which are barely influenced by the confining crystalline regions [3-6].

In this work, the study of the enthalpy relaxation in amorphous and semi-crystalline PLLA is extended to high $(T_g - T_a)$ values, to identify the different scale motions that contribute to physical ageing, and the temperature ranges in which they are active

2.   Experimental Section

PLLA homopolymer (0 % D-lactic acid units) was purchased from Polysciences Inc, U.S.A. The mass-average molar mass (M_w) was approximately 100,000 g mol^{-1}. To avoid degradation of the samples during thermal treatment at high temperatures, PLLA was dried in a vacuum oven at 60 °C for 24 h before use.

A PerkinElmer Differential Scanning Calorimeter DSC 8500, equipped with an IntraCooler III as refrigerating system, was utilized. The instrument was calibrated in temperature with high purity standards materials (indium, naphthalene, cyclohexane) at zero heating rate, according to the procedure for conventional DSC [7].

The PLLA samples were heated from room temperature to 473 K at a rate of 50 K min^{-1}, and maintained at this temperature for 2 min. Subsequently, the samples were either quenched at 323 K and immediately reheated to 368 K at 300 K min^{-1}, to permit cold-crystallization into α'-modification (crystallization time: 90 min), or cooled from 473 K to 408 K at 300 K min^{-1}, to allow melt-crystallization into α-form (crystallization time: 130 min) [8]. At the end of the crystallization, the samples were quenched at 293 K. A completely amorphous sample was also obtained by rapid cooling from 473 K to 293 K. The amorphous and semi-crystalline samples were immediately heated from 293 K to 473 K at 10 K min^{-1}, in order to register the apparent specific heat capacity ($c_{p,app}$) curves, and thus measure the T_g and the amorphous content.

The T_g values were determined as fictive temperature for all the samples [9], which is approximately equivalent to the T_g upon cooling [10]. The weight fraction of the mobile amorphous portion (w_{MAF}) was determined at T_g from the specific heat capacity increment, divided by the Δc_p of the completely amorphous sample; whereas the crystalline weight fraction (w_C) was determined from the area of the exothermal heat flow rate signal detected during the isothermal crystallizations at 368 K and 408 K, divided by the enthalpy of melting of 100% crystalline α'- and α-forms [11]. Finally, the rigid amorphous weight fraction (w_{RAF}) was calculated by difference.

The T_g and the specific heat increment at T_g (Δc_p) for the amorphous and semi-crystalline PLLA samples, together with the respective w_C, w_{MAF} and w_{RAF} values are reported in Table 1. The different glass transition temperatures of PLLA after crystallization at low and high T_cs were connected to the vitrification/devitrification of a slightly constrained and unconstrained mobile amorphous fractions, respectively [12].

Table 1. T_g and specific heat capacity increment at T_g (Δc_p), crystalline (w_C), mobile amorphous (w_{MAF}) and rigid amorphous (w_{RAF}) weight fractions of the amorphous and semi-crystalline PLLA samples investigated. Estimated error: ±0.5 K for T_g, ±0.02 J g⁻¹ K⁻¹ for Δc_p, ±0.02 for w_C and w_{MAF}, ±0.04 for w_{RAF}.

| PLLA	T_g (K)	Δc_p at T_g (J g⁻¹ K⁻¹)	w_C	w_{MAF}	w_{RAF}
amorphous	332.0	0.56	-	1.00	-
T_c = 368 K	342.0	0.20	0.36	0.38	0.26
T_c = 408 K	339.5	0.15	0.43	0.28	0.29
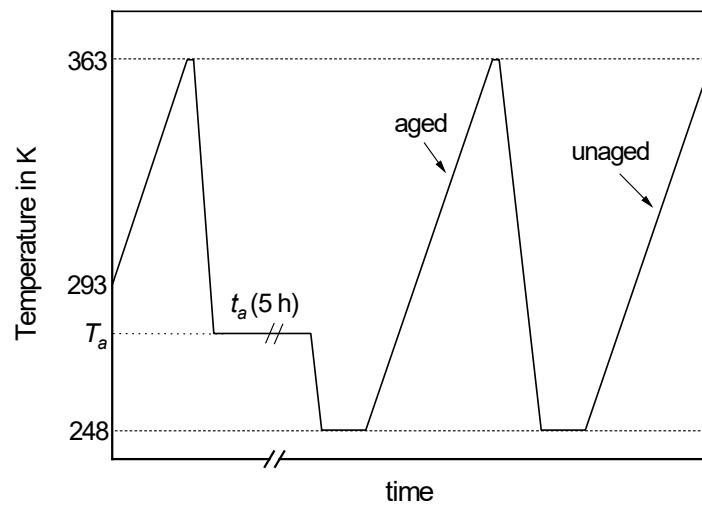
Fig.1 Temperature profile for the enthalpy relaxation experiments

The study of the enthalpy relaxation at different T_as for a fixed ageing time was performed according to the temperature profile shown in Fig. 1. The semi-crystalline PLLA samples were heated to 363 K, kept for 0.3 min at 363 K, and cooled at the fastest available cooling rate to the preselected annealing temperature T_a (average cooling rate: 90 K min⁻¹), included between 281 K and 341 K. The samples were maintained at T_a for t_a = 5 hours, then cooled down to 248 K at the fastest cooling rate

3

(average cooling rate: 60 K min^{-1}). The $c_{p,app}$ curves of the aged samples ($c_{p,app,aged}$) were obtained by heating at 20 K min^{-1} from 248 K to 363 K, whereas the $c_{p,app}$ curves of the unaged samples ($c_{p,app,unaged}$) were achieved, after cooling from 363 K to 248 K at the highest cooling rate, by re-heating from 293 K to 363 K at 20 K min^{-1}. For the amorphous PLLA, T_a was between 273 K and 331 K, with the limit temperature of 363 K reduced to 353 K to prevent crystallization of the sample.

3.   Results and discussion

In order to illustrate the evolution of the apparent specific heat capacity curves after annealing of 5 hours at different T_as, some selected $c_{p,app,aged}$ and the corresponding $c_{p,app,unaged}$ for amorphous PLLA are displayed in Figure 2. The difference between the $c_{p,app,aged}$ and $c_{p,app,unaged}$ curves for amorphous and semi-crystalline PLLA samples ($\Delta c_{p,app} = c_{p,app,aged} - c_{p,app,unaged}$), after annealing at different T_as for 5 hours, was thus derived. Theses $\Delta c_{p,app}$ curves are shown in Figure 3.
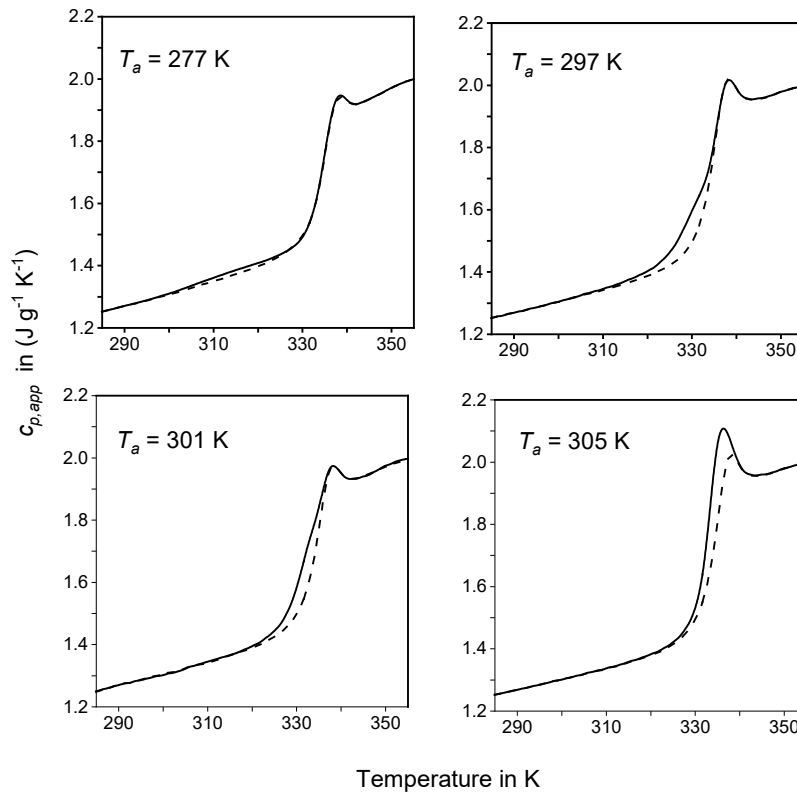

Fig. 2 Apparent specific heat capacity ($c_{p,app}$) curves of aged ($c_{p,app,aged}$, solid line) and unaged ($c_{p,app,unaged}$, dashed line) amorphous PLLA upon heating at 20 K min^{-1}, after annealing of 5 hour at the indicated T_as.

The enthalpy that relaxes during the annealing of a glass at T_a for a period of time t_a, Δh_a (T_a, t_a), recovered during the successive heating run, is determined by integration of the $\Delta c_{p,app}$ curve, according to the following relation [13]:

$$\Delta h_a(T_a, t_a) = \int_{T_1}^{T_2} \Delta c_{p,app} \, dT \qquad (1)$$

where T_1 and T_2 are two temperatures well below and above the glass transition region respectively. In Fig. 2 the $\Delta c_{p,app}$ curves registered after annealing at the lowest investigated T_as are highlighted in red, as better discussed below.
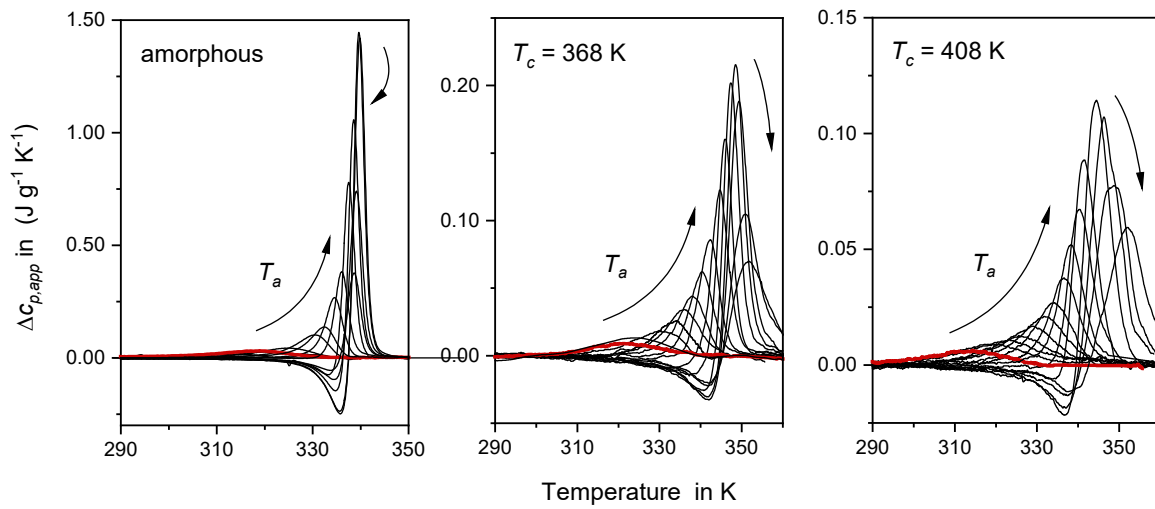
Fig. 3 $\Delta c_{p,app}$ curves of amorphous and semi-crystalline PLLA crystallized at the T_cs indicated after annealing of 5 hour at different T_as. The red solid lines are the $\Delta c_{p,app}$ curves after annealing at the lowest T_as.

Fig. 4(A) displays the enthalpy recovered, Δh_a, as a function of the undercooling ($T_g - T_a$), whereas Fig. 4(B) and 4(C) show the trends of Δh_a after normalization with respect to the overall non-crystalline fraction $(1-w_C) = (w_{MAF} + w_{RAF})$, and the mobile amorphous fraction w_{MAF}, respectively. These curves are almost coincident with those reported in the former study up to the undercooling of about 45 K [1], although a slightly different thermal protocol was here used. Fig. 4(A) reports also the maximum enthalpy, $\Delta h_{a,max}$, that can be lost by the amorphous and semi-crystalline PLLA samples at a given T_a, estimated as $\Delta c_p \cdot (T_g - T_a)$, where Δc_p is the specific heat capacity increment at T_g.
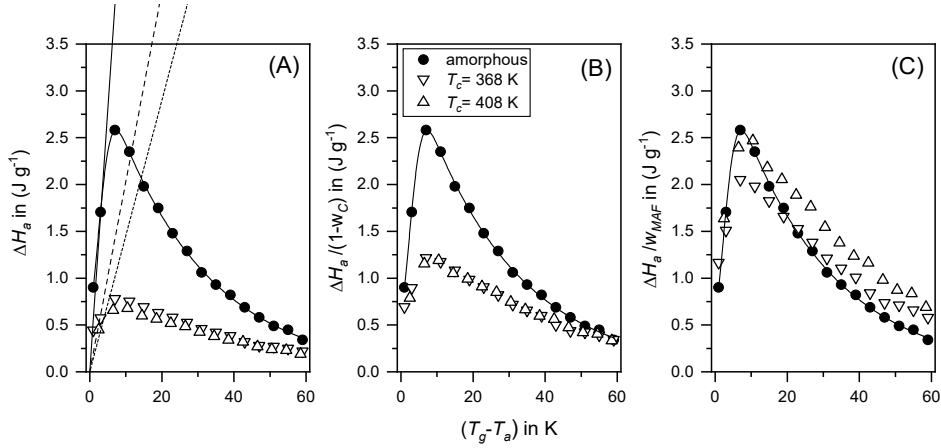
Fig. 4 (A) Reduction in enthalpy (Δh_a), (B) reduction in enthalpy normalized to the total amorphous fraction [$\Delta h_a /(1-w_C)$], (C) reduction in enthalpy, normalized to the mobile amorphous fraction ($\Delta h_a /w_{MAF}$), after 5 hours of annealing for amorphous and semi-crystalline PLLA samples, as a function of (T_g -T_a). The solid line that connects the Δh_a data of the amorphous PLLA is a guide to the eye. The solid, dashed and dotted lines are the maximum enthalpy that can be lost at a given (T_g -T_a) by the amorphous and semi-crystalline PLLA crystallized at 368 K and 408 K, respectively. Estimated error for Δh_a: $\pm$ 0.1 J g^{-1}, for [$\Delta h_a /(1-w_C)$] and ($\Delta h_a /w_{MAF}$): $\pm$0.15 J g^{-1}.

The main finding discussed in the previous work regards the deviation of the $\Delta h_a/w_{MAF}$ data from the amorphous curve at high undercooling. The overestimation of the role of the MAF was considered as a proof that the RAF, which is absent in the amorphous PLLA, also takes part in the enthalpy relaxation. It was suggested that the RAF contribution becomes recognizable with reducing T_a, in parallel with the concomitant decrease in the cooperative segmental motions, which are active during physical ageing only in the MAF regions and primarily at low undercooling [2].

However, the temperature ranges in which the different motions predominantly contribute to the structural relaxation of PLLA were not identified. From this point of view, the present Fig. 4(B) appears very significant, because it reveals that at undercooling higher than 55 K, the relaxed enthalpy normalized to the total non-crystalline fraction [$\Delta h_a/(1-w_C)$] overlaps the amorphous curve. This means that MAF and RAF contribute similarly to structural relaxation at ($T_g -T_a$)> 55 K. This can occur exclusively through localized motions, the only ones active in the rigid amorphous fraction at temperatures below T_g [3-6]. The matching of the Δh_a and [$\Delta h_a/(1-w_C)$] curves for the amorphous and semi-crystalline samples at ($T_g - T_a$)> 55 K indicates that also in amorphous PLLA, structural relaxation originates from local motions at this undercooling. Secondary β-relaxations were indeed found active in amorphous and semi-crystalline PLLA down to about -100 °C [5,14,15].

Figure 3 displays that with reducing T_a, the $\Delta c_{p,app}$ peaks shifts toward temperatures progressively lower. After annealing at the lowest T_as, the $\Delta c_{p,app}$ peaks appear centred at about 20 K below the respective T_gs for the amorphous and semi-crystalline PLLA samples, which proves that

the enthalpy lost during annealing at the highest undercooling investigated is completely recovered below T_g. This confirms that structural relaxation occurs at the highest undercooling via conformational rearrangements that are completely different from the ones responsible for the glass transition process. Also a recent paper on physical ageing of polymers at temperatures far below T_g provided evidence of a mechanism different from the slow one observed close to T_g [16]. The presence of sub-T_g peaks is an event commonly observed in the c_p curves of polymeric glasses physically aged tens of degrees below T_g [17]. The temperature of the sub-T_g peak generally increases with the annealing time, although it was found not to approach the T_g value for progressively increasing undercooling [17].

It is worth noting that for the amorphous PLLA annealed at low T_as, both the $c_{p,app,aged}$ and $c_{p,app,unaged}$ curves exhibit also an enthalpy recovery peak at about 338 K (Figure 2). This second $c_{p,app}$ overshot is ascribable to the enthalpy loss that occurs during the cooling and the heating steps at temperatures close to T_g, where the equilibration rate is high [18]. A double enthalpy recovery in different temperature ranges further attests the difference in the equilibration mechanisms at high and low undercooling.

Several studies demonstrated that the dynamics of the structural relaxation can be described by the Vogel-Fulcher-Tamman (VFT) equation, which is generally used to fit data relative to the cooperative segmental α-relaxation, only in proximity of T_g [19-23], or at undercooling of few degrees [24,25]. With decreasing the annealing temperature, deviations from the VFT law towards a smoother temperature dependence, or an Arrhenius-type behaviour, have been reported [19-23].

Also for PLLA cooperative segmental motions could be the main and more efficient mechanism for structural relaxation close to T_g or at undercooling of few degrees. In this temperature range not far from T_g, the α-relaxation is expected to produce high reduction in enthalpy, due to the large-scale motions that characterize it, which involve the simultaneous rearrangements of several monomeric units. Certainly the faster local motions participate in physical ageing in the whole $(T_g - T_a)$ range investigated, but in the presence of cooperative long-range conformational rearrangements, their contribution can be less important. An investigation on the equilibration time and on the ageing rate as a function of the undercooling might evidence changes in the mechanism that mainly contributes to physical ageing in PLLA. This hypothesis is however to be confirmed, and further studies on this issue are at the moment in progress.

As discussed above, Fig. 4(B) reveals that in PLLA only sub-segmental motions produce structural relaxation at undercooling higher than 55 K in both amorphous and semi-crystalline PLLA. This finding leads therefore to deduce that for $(T_g - T_a)$ values included between the low undercooling at which cooperative segmental motions are active and about 55 K, rearrangements different from

pure large-scale cooperative and pure small-scale local motions contribute to physical ageing in PLLA.

Table 1 shows that for the two semi-crystalline PLLA samples investigated, the RAF content is similar, being the respective values within the experimental error, which means that the contribution of RAF to structural relaxation is also similar. More importantly, the trend of the normalized $\Delta h_a/w_{MAF}$ curves displays that at undercooling higher than about 3 K, the supposed MAF contribution to structural relaxation is higher for the sample crystallized at higher T_c, characterized by a lower T_g, and a higher mobility of the amorphous regions. This suggests that rearrangements involving chain segments of the only MAF region could facilitate structural relaxation in this temperature range, in addition to the RAF contribution, which could be similar in the two semi-crystalline PLLA samples. The different MAF mobility has been suggested to arise from different crystalline morphologies, and consequently different MAF region size [12]. The rearrangements occurring only in the MAF might be intermediate between the large-scale cooperative motions, active at low undercooling, and the small-scale local motions, the only mechanism of equilibration operative at high undercooling.

This interpretation is consistent with the results obtained from previous studies on molecular mobility in semi-crystalline PLLA, performed by dielectric relaxation spectroscopy [15]. A multicomponent character was found for the secondary β-relaxation process, which resulted from the sum of three components with variable contributions as a function of crystallinity [15]. For the slowest β-relaxation, the ratio (E_β/RT_g) is about 21, where $E_\beta = 60$ kJ mol^{-1} is the activation energy [15]. This value is very close to 24, which was found typical of the secondary Johari-Goldstein (JG) relaxation [26]. The JG process is considered a precursor of the cooperative α-relaxation, because at temperatures lower than T_g, it involves the motion of the entire monomeric or structural unit, *via* simultaneous small-scale molecular rearrangements, which do not occur cooperatively with other structural segments [27-29]. Also for some polyesters, such as poly(ethylene terephthalate), poly(ethylene naphthalene dicarboxylate), poly(ethylene isophthalate) and poly(butylene isophthalate), which exhibit different β sub-glass modes, the slowest ones were connected with the JG relaxation [30].

Thus, the existence of simultaneous non-cooperative local motions, involving the whole repeating unit or maybe slightly larger structural portions only in the MAF region, could account partially for the structural relaxation of PLLA at undercooling between about 3 K and 55 K. These associated and extended local motions could be hindered in the RAF layers, due he presence of strong constraints caused by the close crystalline regions. It is worth noting that the JG process has an Arrhenius temperature dependence in the glassy state [29], which is in perfect agreement with the

deviations from the VFT law found for progressively decreasing annealing temperatures in previous ageing studies [19-23]. Also the JG process is expected to progressively slow down by reducing the annealing temperature, so that at undercooling higher than 55 K, exclusively local motions become the main cause for the structural relaxation in PLLA.

4.   Conclusions

The contribution of different motions to structural relaxation of PLLA has been identified by comparing the enthalpy recovered after isochronal annealing at different temperatures for amorphous and semi-crystalline samples. Undercooling limit of about 55 K, below which exclusively small-scale localized motions produce structural relaxation in both amorphous and semi-crystalline PLLA has been identified. In addition, motions different from pure cooperative large-scale motions and pure small-scale local rearrangements, localized in the MAF, are found to mainly contribute to structural relaxation at intermediate undercooling. These motions are suggested to be related to the Johari-Goldstein process.

The study has demonstrated that in semi-crystalline PLLA, both MAF and RAF participate in structural relaxation: MAF is supposed to contributes (*i*) close to T_g, with cooperative large-scale motions, (*ii*) at intermediate undercooling, with simultaneous and associated non-cooperative local motions, involving the entire structural unit, (*iii*) at high undercooling, exclusively with small-scale localized motions. The contribution of the RAF, which is generated by small-scale local motions in the whole undercooling range investigated, becomes recognizable by reducing T_a, in parallel with the concomitant disappearance of the cooperative segmental motions, and the progressive reduction in non-cooperative associated local motions.

References

[1]   B. Wunderlich, Reversible crystallization and rigid-amorphous phase in semi-crystalline macromolecules, Progr. Polym. Sci. 28 (2003) 383-450.

[2]   M.C. Righetti, M. Gazzano, N. Delpouve, A. Saiter, Contribution of the rigid amorphous fraction to physical ageing of semi-crystalline PLLA, Polymer 125 (2017) 241-253.

[3]   J. Dobbertin, A. Hensel, C. Schick, Dielectric spectroscopy and calorimetry in the glass transition region of semi-crystalline poly(ethylene terephthalate), J. Thermal Anal. 47 (1996) 1027-1040.

[4]   C. Schick, J. Dobbertin, M. Potter, H. Dehne, A. Hensel, A. Wurm, A.M. Ghoneimm S. Weyer, Separation of components of different molecular mobility by calorimetry, dynamic mechanical and dielectric spectroscopy, J. Thermal Anal. 49 (1997) 499-511.

[5]   J. Ren, K. Adachi, Dielectric relaxation in blends of amorphous poly(DL-lactic acid) and semicrystalline poly(L-lactic acid), Macromolecules 36 (2003) 5180-5186.

[6]   A. Schönals, Molecular Dynamics in Polymer Model Systems in: F. Kremer, A. Schönals (Eds.), Broadband Dielectric Spectroscopy, Springer-Verlag Berlin, Germany, 2003, pp. 225-293.

[7]   S.M. Sarge, W. Hemminger, E. Gmelin, G.W.H. Höhne, H.K. Cammenga, W. Eysel, Metrologically based procedures for the temperature, heat and heat flow rate calibration of DSC, J. Therm. Anal. 49 (1997) 1125-1134.

[8]   P. Pan, W. Kai, B. Zhu, T. Dong, Y. Inoue, Polymorphous crystallization and multiple melting behavior of poly(L-lactide): molecular weight dependence, Macromolecules 40 (2007) 6898-6905.

[9]   M.J. Richardson, N.G. Savill, Derivation of accurate glass transition temperatures by differential scanning calorimetry, Polymer 16 (1975) 753-757.

[10] E. Lopez, S.L. Simon, Signatures of structural recovery in polystyrene by nanocalorimetry, Macromolecules 49 (2016) 2365-2374.

[11] M.C. Righetti, M. Gazzano, M.L. Di Lorenzo, R. Androsch, Enthalpy of melting of α'- and α-crystals of poly(L-lactic acid), Eur. Polym. J. 70 (2015) 215–220.

[12] M.C. Righetti, D. Prevosto, E. Tombari, Time and temperature evolution of the rigid amorphous fraction and differently constrained amorphous fractions in PLLA, Macromol. Chem. Phys. 217 (2016) 2013-2026.

[13] S.E.B. Petrie, Thermal behavior of annealed organic glasses, J. Polym. Sci Part A-2: Polym. Phys. 10 (1972) 1255-1272.

[14] A.R. Bras, M.T. Viciosa, Y. Wang, M. Dionisio, J.F. Mano, Crystallization of poly(L-lactic acid) probed with dielectric relaxation spectroscopy, Macromolecules 39 (2006) 6513-6520.

[15] A.R. Bras, P. Malik, M. Dionisio, J.F. Mano, Influence of crystallinity in molecular motions of poly(L-lactic acid) investigated by dielectric relaxation spectroscopy, Macromolecules 41 (2008) 6419-6430.

[16] N.G. Perez-De Eulate and D. Cangialosi, The very long-term physical ageing of glassy polymers, Phys. Chem. Chem. Phys. 20 (2018) 12356.

[17] A.R. Berens, I.M. Hodge, Effects of annealing and prior history on enthalpy relaxation in glassy polymers. 1. Experimental study on poly(vinyl chloride), Macromolecules 15 (1982) 756-761.

[18] S. Montserrat, Physical aging studies in epoxy resins. I. Kinetics of the enthalpy relaxation process in a fully cured epoxy resin, J. Polym. Sci. Polym. Phys. 32(1994) 509–522.

[19] D. Cangialosi, V.M. Boucher, A. Alegria, J. Colmenero, Physical ageing in polymers and polymer nanocomposites: recent results and open questions, Soft Matter 9 (2013) 8619-8630.

[20] G.B. McKenna and S.L. Simon, 50th Anniversary perspective: challenges in the dynamics and kinetics of glass-forming polymers, Macromolecules 50 (2017) 6333-6361.

[21] P.A. O'Connell, G.B. McKenna, Arrhenius-type temperature dependence of the segmental relaxation below T_g, J. Chem. Phys. 110 (1999) 11054-11060.

[22] S. L. Simon, J. W. Sobieski and D. J. Plazek, Volume and enthalpy recovery of polystyrene, Polymer, 2001, 42, 2555–2567.

[23] J. Zhao, G.B. McKenna, Temperature divergence of the dynamics of a poly(vinyl acetate) glass: Dielectric vs. mechanical behaviors, J. Chem. Phys. 136 (2012) 154901.

[24] H. Wagner, R. Richer, Dielectric relaxation of the electric field in poly(vinyl acetate): a time domain study in the range 10^{-3}-10^{-6} s, Polymer 38 (1997) 255-261.

[25] V.M. Boucher, D. Cangialosi, A. Alegria, J Colmenero, Time dependence of the segmental relaxation time of poly(vinyl acetate) – silica nanocomposites, Phys. Rev. E. 86 (2012) 041501.

[26] K.L. Ngai, S. Capaccioli, Relation between the activation energy of the Johari-Goldstein β relaxation anf T_g of glass formers, Phys. Rev. E 69 (2004) 031501.

[27] G.P. Johari, M. Goldstein, Viscous liquids and the glass transition. III. Secondary relaxations in aliphatic alcohols and other nonrigid molecules, J. Chem. Phys. 55 (1971) 2372-2388.

[28] G.P. Johari, Intrinsic mobility of molecular glasses, J. Chem. Phys. 58 (1973) 1766.

[29] K.L. Ngai, M. Paluch, Classification of secondary relaxation in glass-formers based on dynamic properties, J. Chem. Phys. 120 (2004) 857-873.

[30] A. Nogales, A. Sanz, T.A. Ezquerra, On the role of the β process as precursor of the α relaxation in aromatic polyesters, J. Non-Cryst. Solids 352 (2006) 4649-4655.